PHYSICAL REVIEW B **77**, 094123 (2008)

Equation of state of gallium oxide to 70 GPa: Comparison of quasihydrostatic and nonhydrostatic compression

Kristina E. Lipinska-Kalita,[1] Patricia E. Kalita,[2,*] Oliver A. Hemmers,[3] and Thomas Hartmann[4]
[1]*Department of Chemistry, University of Nevada Las Vegas, 4505 Maryland Parkway, Box 454003, Las Vegas, Nevada 89154-4003, USA*
[2]*Department of Physics, University of Nevada Las Vegas, 4505 Maryland Parkway, Box 4002, Las Vegas, Nevada 89154-4002, USA*
[3]*Office of Strategic Energy Programs and Department of Chemistry, University of Nevada Las Vegas, 4505 Maryland Parkway, Box 454003, Las Vegas, Nevada 89154-4003, USA*
[4]*Idaho National Laboratory and College of Engineering, Idaho State University, Campus Box 8060, Pocatello, Idaho 83209, USA*
(Received 8 August 2007; revised manuscript received 14 October 2007; published 19 March 2008)

Synchrotron x-ray diffraction and diamond-anvil cell techniques were used to characterize pressure induced structural modifications in gallium oxide. Gallium oxide was studied on compression up to 70 GPa and on the following decompression. The effect of the pressure-transmitting medium on the structural transformations was investigated in two sets of compression and decompression runs, one with nitrogen as a quasihydrostatic pressure-transmitting medium and the other in nonhydrostatic pressure conditions. The x-ray diffraction data showed gradual phase transition from a low-density, monoclinic β-Ga_2O_3 to a high-density, rhombohedral α-Ga_2O_3. With the use of nitrogen as a pressure transmitting medium, the β- to α-Ga_2O_3 transition begins at about 6.5–7 GPa and extends up to ~40 GPa, confirming recent theoretical calculations. This pressure-driven transition is irreversible and the material decompressed from 70 GPa to ambient conditions was composed, in both sets of experimental runs, of α-Ga_2O_3 only. A Birch-Murnaghan fit of the unit cell volume as a function of pressure yielded a zero pressure bulk modulus $K_0=199(6)$ GPa, and its pressure derivative $K_0'=3.1(4)$ for theβ-Ga_2O_3 phase, and $K_0=220(9)$ GPa and $K_0'=5.9(6)$ for the α-Ga_2O_3 phase for the experiments performed in quasihydrostatic compression conditions. When for the same experiment K_0' is held at 4, then the bulk modulus values are 184(3) and 252(14) GPa for β-Ga_2O_3 and the α-Ga_2O_3, respectively. We compare the results of this work with our previous studies on the high-pressure behavior of nanocrystalline gallium oxide.

DOI: 10.1103/PhysRevB.77.094123 PACS number(s): 61.46.−w, 61.05.cp, 62.50.−p, 64.30.−t

I. INTRODUCTION

Bulk gallium oxide belongs to the group of transparent oxides with the widest band gap ($E_g \sim 4.9$ eV) and displays tunable optical, magnetic and electronic properties.[1,2] The compound exhibits both conduction and luminescence properties and thus attracts much research interest due to numerous technological applications.[2–11] The number of oxygen vacancies present in this material depends on the growth atmosphere, and determines the electrical character of the compound, which can vary, in a tunable way, from insulating to conductive. When prepared under reducing conditions, gallium oxide becomes an *n*-type semiconductor, due to oxygen vacancies. Polycrystalline semiconducting Ga_2O_3 thin films represent promising materials for gas sensor devices. Recently it was proposed that gas molecules can be dissociatively adsorbed by oxygen deficient sites on the β-Ga_2O_3 surface.[12] Furthermore, the magnetism of the conduction electron spins in this material exhibits an original memory effect from 4 K to at least room temperature and could be exploited in the field of magnetic memory devices.[10,11]

In ambient conditions, the thermodynamically stable form of gallium oxide is the monoclinic structure of β-Ga_2O_3. However, the compound shows polymorphism and depending on temperature-pressure-atmosphere conditions, can appear in five different stable or metastable crystal structures (α, β, γ, δ, ε).[2,8,9]

This work is part of our extensive project on optically transparent nanocomposites based on dielectric matrices, doped by nanocrystals.[13–19] In a previous work on nanocrystalline composites, Lipinska-Kalita *et al.*[14] reported a pressure-induced β-Ga_2O_3 to α-Ga_2O_3 phase transition, starting at about 6 GPa, in nanocrystalline gallium oxide (*nc*-Ga_2O_3) embedded in an amorphous silica host network. That work inspired our extended high-pressure investigations of bulk, crystalline gallium oxide. We demonstrated a β- to α-Ga_2O_3 phase transition[20,21] occurring in bulk gallium oxide in different pressures ranges, starting below ~10 GPa and dependent on the conditions of the compression experiment.

In this paper, we present comprehensive results of our high-pressure work on bulk crystalline β-Ga_2O_3, including compression to 70 GPa followed by gradual decompression to ambient pressure. The experiments were performed in both quasihydrostatic as well as nonhydrostatic pressure conditions. To the best of our knowledge, this is the first investigations of equation of state of gallium oxide based on synchrotron x-ray diffraction and on *in situ* compression up to 70 GPa.

II. EXPERIMENT

A sample of gallium oxide of 99.99% purity was obtained from Alfa Aesar. The original material was only partly crystalline and in order to transform it into a fully crystalline form, it was annealed for several hours at an elevated temperature. The resulting material was completely crystalline

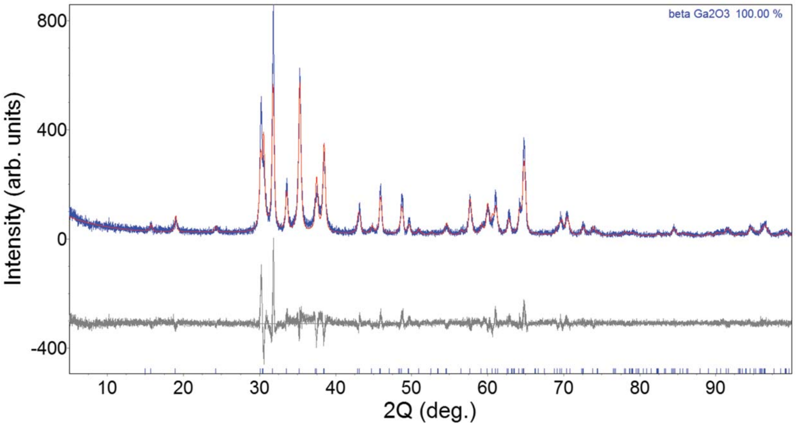

FIG. 1. (Color online) Full profile Rietveld structural refinement of β-Ga_2O_3 used for high-pressure studies. The fit has an $R_{wp}=1.8$ and the calculated intensities match well the observed intensities. Red, blue, and black solid lines represent experimental, calculated, and difference pattern, respectively. The pattern was collected in ambient pressure and temperature conditions using CuK_α radiation.

and a structural refinement confirmed it to be the monoclinic form, corresponding to β-Ga_2O_3.

Conventional angle dispersive x-ray diffraction patterns were collected in θ-2θ Bragg-Brentano geometry, using a PANalytical X'Pert PRO x-ray diffractometer with Cu K_α radiation (40 kV, 40 mA) and an X'Celerator solid state detector. The patterns were recorded with a step size of $0.008°2\theta$ in the range 5° to $100°2\theta$ and 24 s per step.

In situ angle dispersive synchrotron x-ray diffraction studies were performed on compression up to 70 GPa and successive decompression to ambient pressure. In order to analyze the effects of uniaxial stresses on the structural transformations of gallium oxide we performed four runs of experiments, involving compression and decompression, using a diamond-anvil cell (DAC) with the sample loaded either without a pressure-transmitting medium or with nitrogen serving as a quasihydrostatic pressure-transmitting medium. For synchrotron x-ray diffraction studies the powdered sample was compressed in a Mao-Bell-type DAC using diamonds with 300 μm diameter culets. The sample chamber consisted of a 90 μm diameter hole drilled in a rhenium gasket, preindented to a thickness of 40 μm. Pressure was determined as an average of the reading from three ruby chips dispersed in the sample chamber and the pressure scale of Mao[22] was used. The time interval between each pressure increase (compression) or each pressure decrease (decompression) was about 20 min. The time interval between the compression sequence and the decompression sequence was about 30 days. All x-ray diffraction patterns were collected at the 16-ID-B undulator beamline at the High Pressure Collaborative Access Team (HPCAT), sector 16, Advanced Photon Source, Argonne National Laboratory, using a monochromatic synchrotron radiation source of 0.3680, 0.4057, or 0.4007 Å. Diffraction images were recorded using a MAR345 imaging plate as an area detector and were integrated and corrected for distortion using the FIT2D software.[23] The average acquisition time was 10 sec. The sample-detector distance and geometric parameters were calibrated using a CeO_2 standard from NIST. The 10 μm $\times 15$ μm x-ray beam was achieved by microfocusing with two Kirckpatrick-Baez mirrors and a 30 μm diameter Mo cleanup pinhole to eliminate the beam tails. Indexing, least squares lattice parameters refinements and Rietveld full profile structural refinements were done with the use of POWDER CELL[24] and TOPAS 2.1.[25]

III. RESULTS

A conventional, angle-dispersive x-ray diffraction pattern of gallium oxide was collected to determine lattice parameters of the compound at ambient pressure and temperature. A Rietveld refinement confirmed the identity of the compound to be the monoclinic β-Ga_2O_3 (space group $C2/m$). The pattern together with its Rietveld full profile refinement is shown in Fig. 1. The fit accounts for all the lines present and has an $R_{wp}=1.8$. Minor discrepancies between observed and calculated line intensities could be explained by a certain degree of structural disorder and nonstoichiometry caused by the reported oxygen vacancies.[5–9] The refined β-Ga_2O_3 lattice parameters are $a=12.233(10)$ Å, $b=3.038(3)$ Å, $c=5.807(5)$ Å, $\beta=103.821(7)°$, with cell volume $V=209.56(4)$ Å^3, and x-ray density $d=5.941(9)$ g/cm^3.

Two high-pressure compression and decompression runs were carried out in order to compare the effect of the pressure-transmitting medium on the high-pressure behavior of β-Ga_2O_3. In the first set of experiments nitrogen was used as a quasihydrostatic pressure medium. The evolution of synchrotron x-ray diffraction patterns in the compression run up to 70 GPa and the following decompression run to ambient pressure, with nitrogen as pressure medium, is shown in Figs. 2(a) and 2(c). The second run of compression and decompression experiments was performed without a pressure medium and the corresponding synchrotron x-ray diffraction patterns are shown in Figs. 2(b) and 2(d). For both experimental runs, the low pressure patterns consist of several sharp Bragg lines with narrow bandwidth, which correspond well to the β phase of Ga_2O_3. With increase of pressure, the diffraction lines shift towards higher 2θ angles (lower d spacings), relative intensities change and some Bragg lines disappear while new lines emerge. In both experiments, the diffraction patterns indicate a progressive, pressure-driven phase transition from monoclinic (β-Ga_2O_3) to rhombohedral (α-Ga_2O_3) gallium oxide, with a wide transition pressure range where the two phases coexist. At 70 GPa, the only remaining phase is the α-Ga_2O_3 [Figs. 2(a) and 2(b)]. All patterns of the decompression sequence show lines of only

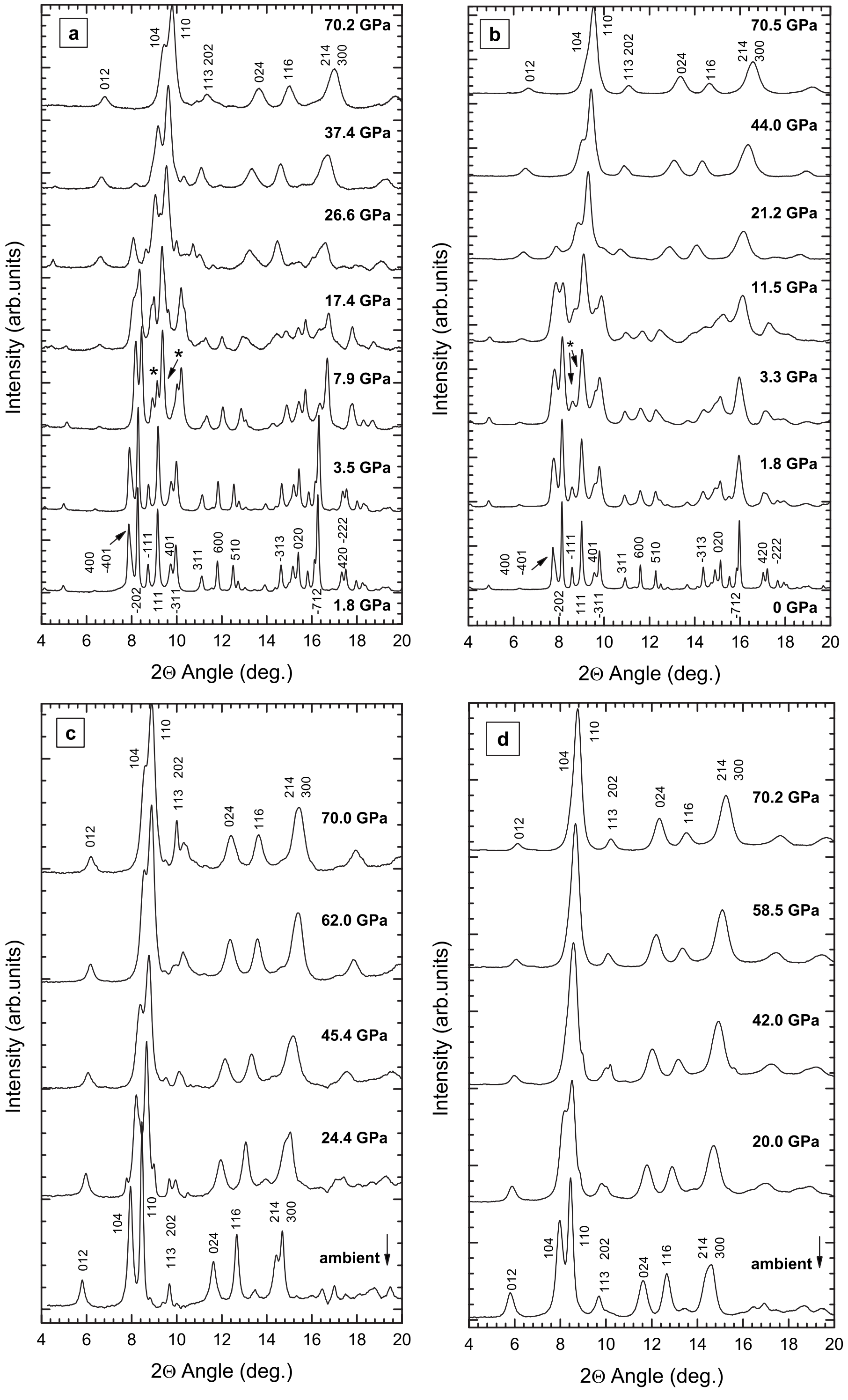

FIG. 2. Selected angle-dispersive synchrotron x-ray diffraction patterns collected in the diamond-anvil cell in compression up to 70 GPa and subsequent decompression: (a) compression with nitrogen as pressure transmitting medium, (b) compression of neat sample, (c) decompression with nitrogen as pressure transmitting medium, (d) decompression of neat sample. The *hkl*'s are indicated for both phases. Stars mark the appearance of the new diffraction peaks of the α-phase overlapping with the β-phase or the enhancement of scattering background due to the onset of the phase transition. The pressure-induced phase transition is irreversible and upon complete pressure release: both (c) and (d) are constituted of the α-Ga_2O_3 phase only.

the α phase [Figs. 2(c) and 2(d)] and the gradual shift of all diffraction lines towards lower 2θ angles indicates a progressive relaxation of the α structure. A complete pressure release to ambient conditions demonstrates that the pressure-driven β-Ga_2O_3 to α-Ga_2O_3 phase transition is not reversible.

The x-ray diffraction patterns of both compression runs [Figs. 2(a) and 2(b)] show different degrees of pressure-induced line broadening due to uniaxial stresses created by nonhydrostatic conditions in the DAC. The patterns of compression without pressure-transmitting medium [Fig. 2(b)], show a pronounced line broadening in all but the very first pattern. When nitrogen is employed as a pressure medium [Fig. 2(a)], however, quasihydrostatic conditions are ensured in the pressure range where the phase-transition begins. Line broadening only starts to be noticeable at much higher pressures (~17 GPa and above), as a consequence of inhomogeneous effects of increasing nonhydrostatic stresses in the DAC. Upon decompression to ambient conditions, the effect of the pressure medium is reflected by the much narrower

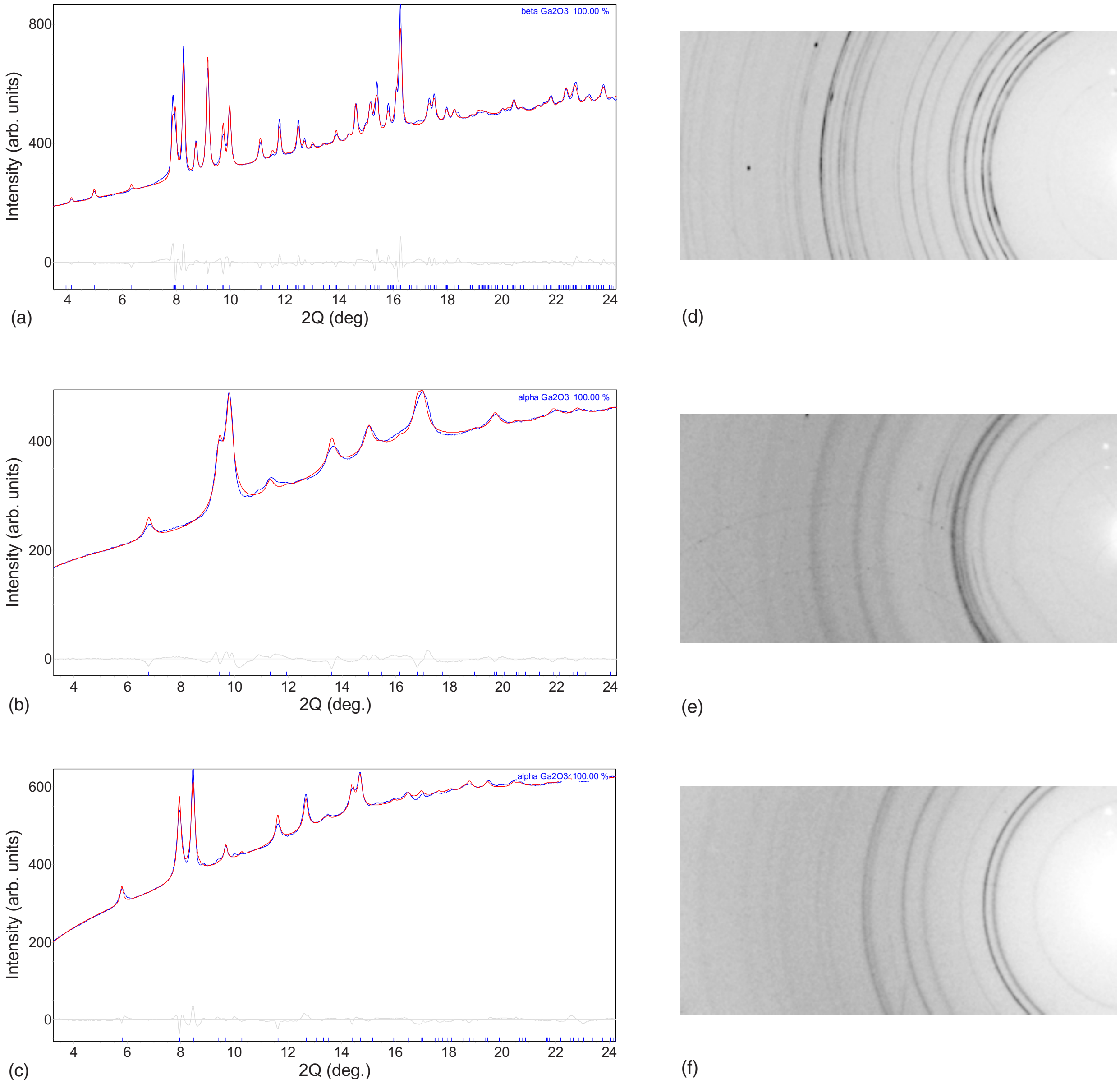

FIG. 3. (Color online) Left: Rietveld full-profile refinements of the diffraction patterns collected on compression: at 1.8 GPa (a) with β-Ga_2O_3 phase only, at 70.2 GPa (b), where the refinement revealed a complete transformation of the monoclinic β-Ga_2O_3 into the rhombohedral α-Ga_2O_3 phase, and (c) after decompression to ambient pressure with the α-Ga_2O_3 phase only. Right: the corresponding pictures of the image plate showing powder diffraction rings, illustrating the progress of the phase transition: (d) at 1.8 GPa, (e) at 70.2 GPa, and (f) decompressed to ambient pressure. All data are for gallium oxide compressed with nitrogen as pressure-transmitting medium. Red, blue, and black solid lines represent experimental, calculated and difference patterns, respectively. All fits are good, with an R_{wp} between 2.1 and 4.1.

diffraction lines in the pattern of the sample decompressed with nitrogen as a pressure medium [Fig. 2(c)] than that of the material studied without the pressure medium [Fig. 2(d)].

IV. DISCUSSION

In its ambient pressure and temperature form β-Ga_2O_3 has four formula units in the unit cell, belongs to the space group $C2/m$ (12) and has a monoclinic crystal lattice. The compound contains both octahedral and tetrahedral gallium sites in equal quantities and arranged in parallel chains along the b axis, with oxygens arranged in a distorted-cubic close-packed array.[26–29] A Rietveld full-profile refinement of a diffraction pattern at 1.8 GPa, the first pattern collected on compression using nitrogen as a pressure-transmitting medium, together with the corresponding picture of the image plate is shown in Figs. 3(a) and 3(d). This pattern confirmed the presence of only β-Ga_2O_3 and yielded the following unit cell parameters: $a=12.179(5)$ Å, $b=3.027(1)$ Å, $c=5.782(2)$ Å, $\beta=103.74(1)°$, with $V=207.06(1)$ Å^3 and $d=6.013(9)$ g/cm^3.

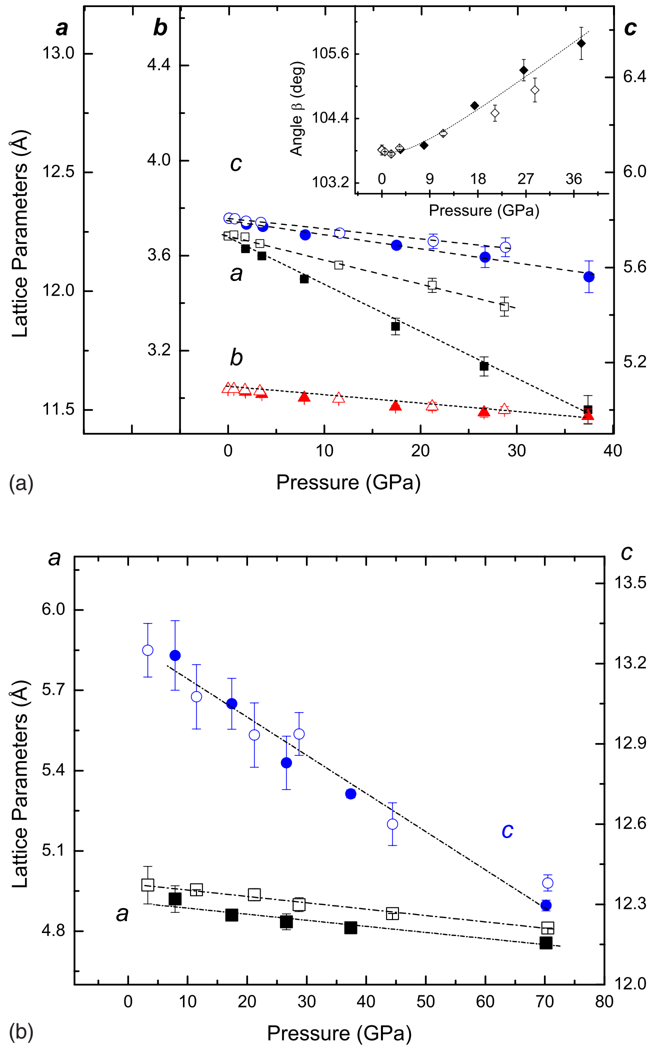

FIG. 4. (Color online) Pressure evolution of the unit cell parameters: (a) of the β-Ga_2O_3 phase and (b) for the α-Ga_2O_3 phase. Black squares represent the a lattice parameter, red triangles the b lattice parameter and blue circles the c lattice parameter. Full symbols refer to the compression with pressure medium and open symbols refer to the compression of neat sample. The inset in plate (a) shows the evolution of the β angle of the β-Ga_2O_3 phase. For the compression with nitrogen as pressure medium: in the case of β-Ga_2O_3 phase the compressibility for the a, b, and c parameters is 6.0, 3.7, and 4.2 %, respectively, the β angle increases by 1.9%; in the case of α-Ga_2O_3 phase the compressibility of the a and c parameters is 3.3 and 7.1 %, respectively. The differential (in Å) of the three vertical scales is the same, in order to facilitate comparison between the evolution of lattice parameters. Dashed lines are drawn as a guide for the eye.

In order to estimate the pressure range of the low-to-high density β- to α-Ga_2O_3 phase transition and to determine the lattice parameters, Rietveld full profile refinements were performed on selected compression patterns and two examples of refinements are shown in Figs. 3(b) and 3(c). The results of the refinements are summarized in the following figures: the pressure evolution of the lattice parameters of the β-Ga_2O_3 is presented in Fig. 4(a) while that of the α-Ga_2O_3 is shown in Fig. 4(b). The lattice compression of both gallium oxide phases is anisotropic, with the a axis being more compressible than the b and c axis in the monoclinic β structure [Fig. 4(a)] and with the c axis being more compressible than the a axis in the rhombohedral α structure [Fig. 4(b)].

The synchrotron x-ray diffraction patterns up to about 7 GPa [Fig. 2(a)], for the compression with nitrogen as a pressure medium, can be well explained with the β-Ga_2O_3 structure only. However, the pattern at 7.9 GPa displays notable changes. Two new diffraction lines appear in the 2θ range 8–10° and they are assigned to the new α-Ga_2O_3 phase: the (104) line and the (110) line, overlapped with the (111) line of the still dominating β-Ga_2O_3 phase [Fig. 2(a)]. The α-Ga_2O_3 phase has a rhombohedral lattice and belongs to the space group R-3c (167) with six Ga_2O_3 in the unit cell. The oxygen ions are positioned in a hexagonal close-packed array and all of the Ga^{3+} ions are octahedrally coordinated to oxygens. The α- to β-Ga_2O_3 phase transition involves an increase of the gallium coordination number from four to six as well as a packing increase through an ~8% volume collapse near 7.9 GPa. At that pressure the amount of the α phase is about 7 wt. % as estimated from Rietveld full-profile refinement. The β- to α-Ga_2O_3 phase transition begins below 7.9 GPa but the β phase dominates the diffraction patterns up to about 20 GPa, and traces of this phase are present up to about 40 GPa. At the final pressure of compression 70.2 GPa, the diffraction pattern is constituted from lines of the α-Ga_2O_3 phase only [Figs. 2(a), 3(b), and 3(e)] and the structural refinement yields the following cell parameters: $a=4.76(1)$ Å, $c=12.30(2)$ Å, with $V=241.4(9)$ Å^3, and $d=7.74(6)$ g/cm^3.

It should be pointed out here that based on the Rietveld refinements, which indicated that at 7.9 GPa, the amount of the alpha phase is already ~7 wt. %, we can extrapolate that the phase transition begins earlier, and more precisely between 6.5 and 7 GPa. However one must keep in mind that the reliability of the phase percentage figure is lower than the error produced by the refinement program and the phase percentage is in fact about 7 ± 3 wt. %. The large error margin originates from the fact that a texture model was introduced to the calculated pattern in order to account for the preferred orientation. Therefore all the phase percentage figures given here have to be considered with caution.

For the compression without a pressure-transmitting medium, only the patterns below 3 GPa [Fig. 2(b)] could be fitted with pure β-Ga_2O_3. Above ~3 GPa we observe the emergence of a high-pressure α-Ga_2O_3 phase. This is evidenced by a change in relative intensities of the diffraction lines accompanied by an increase of background in the 2θ region from 8.5° to 9.5° [Fig. 2(b)]. At this stage of the compression there are no resolved peaks due to the α phase. In fact, the strongest lines of the α-Ga_2O_3, the (104) and (110), are overlapped with the equally strong reflections of the still dominating β phase, the (−111) and (111). The 3.3 GPa pattern [Fig. 2(b)] is additionally broadened due to stresses in the DAC. The Rietveld refinement of this pattern yielded a β- to α-phase mixture ratio of 96:4 in wt. %, and a ~10% volume collapse across the phase transition. As in the previous case, the β-Ga_2O_3 phase dominates the diffraction patterns up to about 12 GPa [Fig. 2(b)] and traces of this phase can be detected up to about 30 GPa. At the final pressure of compression 70.5 GPa, the diffraction pattern is composed entirely from lines of the α-Ga_2O_3 [Fig. 2(b)].

It has to be pointed out that, in both compression runs, with and without pressure-transmitting medium [Figs. 2(a) and 2(b)], the diffraction lines attributed to the new α-Ga_2O_3 structure are, for the most part, not well isolated. At low pressures, they overlap with the lines of the β phase, but their presence is indicated by an enhancement of intensity and profile broadening of those lines. As pressure is raised, however, the amount (as estimated from refinements) of the α phase increases while that of the β phase decreases, and the Bragg lines of the α phase substitute progressively those of the β phase [Figs. 2(a) and 2(b)]. Finally, at the highest investigated pressures, only the α phase is present, which is confirmed by full-profile structural refinements. It is also noteworthy that in both compression runs, the material does not become amorphous at 70 GPa, the highest compression pressure.

In summary, for both runs, the pressure-driven shift of diffraction lines indicates a progressive densification of the β-Ga_2O_3 phase, followed by a gradual transition to the α-Ga_2O_3 phase and further densification of this new phase. The β and α phases coexist across a wide pressure range. This reconstructive, low-to-high-density phase transition with an increase of coordination number of gallium is accompanied by a change in oxygen arrangement from distorted-cubic to trigonal. We conclude that the large coexistence region of the two gallium oxide phases in a homogeneous sample, as well as the reconstructive character of this phase transition could be due to hysteresis arising from nucleation barriers to a first order transition.

The highest pressure of the compression was ~70 GPa in both experimental runs and the reversibility of β- to α-Ga_2O_3 phase transition was followed in the decompression sequence [Figs. 2(c) and 2(d)] down to ambient pressure. At ~70 GPa the diffraction peaks of the denser, high-pressure α-Ga_2O_3 phase are broadened compared with those for α-Ga_2O_3 collected at lower pressures in the decompression run, indicating that a high degree of pressure-induced structural disorder was present at the highest compression pressure (~70 GPa). Figures 3(b) and 3(c) illustrate Rietveld full-profile structural refinements of the patterns of the sample compressed to 70 GPa and decompressed back to ambient conditions, while Figs. 3(e) and 3(f) show the corresponding pictures of the image plate. The refinement yielded the following unit cell parameters: $a=4.979(10)$ Å, $c=13.432(28)$ Å, with $V=288.4(12)$ Å^3, and $d=6.48(3)$ g/cm^3.

In analogy to what was observed in the compression run, the decompression patterns of the material studied without pressure-transmitting medium, displayed considerable line broadening. For the material decompressed from ~70 GPa to ambient conditions the full-width at half-maximum (FWHM) values are ~0.3° 2θ and ~0.2° 2θ for the runs without and with pressure-transmitting medium, respectively, while for β-Ga_2O_3 before compression, the FWHM was ~0.1° 2θ. Such broadening of the diffraction lines is due to more pronounced pressure gradients, uniaxial and shear stresses that arise in the absence of a pressure-transmitting medium.[29] The DAC is essentially an uniaxial stress producing device and truly hydrostatic conditions are only obtained when the sample is contained within a fluid pressure medium.[30] At room temperature, however, a completely hydrostatic environment cannot be sustained above ~13 GPa due to solidification of all known pressure media including helium.[30–32] The liquid and solid nitrogen used to transmit pressure to gallium oxide in these experiments provided quasi-hydrostatic conditions at least to 12 GPa (Ref. 33) but in compression without pressure medium, nonhydrostatic conditions set in from the beginning of the compression run. It has been shown that shear stresses,[30–34] in addition to high pressure, can result in a reduction of the pressure of the onset of a phase transition. In gallium oxide compressed without pressure medium the phase transition starts earlier (at about 3 GPa) and the pressure range of the transition spans over more than 25 GPa. For the sample compressed with nitrogen, the transition starts at about 7 GPa, and the estimated coexistence of the two gallium oxide phases is of more than 30 GPa.

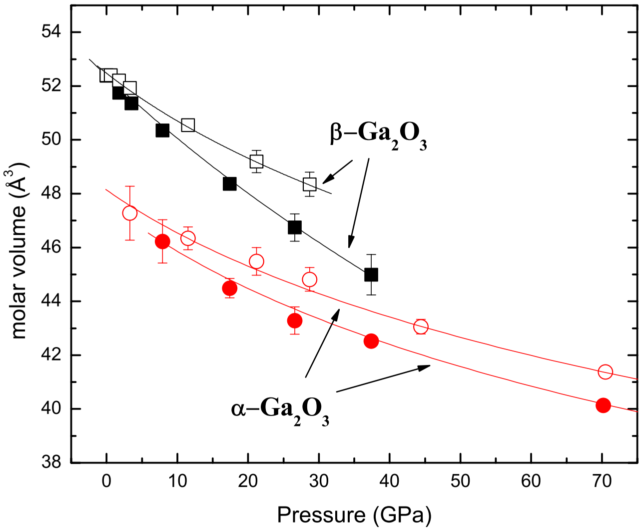

FIG. 5. (Color online) Equations of state (EOS) for the β- and α-phases of gallium oxide. Solid curves are the Birch-Murnaghan EOS fits to the experimental data. Squares represent the molar volume for β-Ga_2O_3 and circles represent the molar volume for α-Ga_2O_3. Solid symbols indicate the experiments performed with nitrogen as quasihydrostatic, pressure-transmitting medium, and open symbols correspond to the experiments performed on the neat sample.

Our findings, which indicate the beginning of the β- to α-Ga_2O_3 phase transition to be between 3 and 7 GPa depending on the pressure medium, are in agreement with recent theoretical calculations by Kroll[35] and by He *et al.*[36] Kroll[35] demonstrates that the monoclinic form of β-Ga_2O_3, the structure with lowest enthalpy, is stable only to about 2.6 GPa. Depending on whether the calculations treat the d electrons of Ga as core or as valence states, gallium oxide is expected to undergo a phase transition from monoclinic form of β-Ga_2O_3 into the corundum-type modification of α-Ga_2O_3 at about 2.6 or 6 GPa, respectively. Also first principles studies of the structural properties of Ga_2O_3 by He *et al.*[36] determined the β-Ga_2O_3 to α-Ga_2O_3 phase transition pressure to be 9.5 GPa (Table I).

TABLE I. Bulk modulus K_0, its pressure derivative K_0' and the unit cell volume at ambient conditions V_0 obtained from fitting the third order Birch-Murnaghan equation of state to the gallium oxide experimental data up, to 70 GPa, for two experimental runs. The pressure of the onset of the β- to α-Ga_2O_3 phase transition is also shown. For comparison reason data for nanocrystalline gallium oxide, *nc*-β-Ga_2O_3 embedded in a glass matrix, from our previous work (Ref. 14) are shown alongside the results of an experimental study up to 38.6 GPa (Ref. 40) as well as the results of theoretical calculation (Refs. 35 and 36).

	β-Ga_2O_3			α-Ga_2O_3			Beginning of $\beta \rightarrow \alpha$ transition
	K_0 (GPa)	K_0'	V_0 (Å^3)	K_0 (GPa)	K_0'	V_0 (Å^3)	
with nitrogen	199(6)	3.1(4)	209.1(2)	220(9)	5.9(6)	288(1)	~6.5–7 GPa
	184(3)	4	209.4(2)	252(14)	4	288(1.5)	
neat sample	255(16)	7.63(90)	209.9(4)	261(20)	7.93(71)	288.8(1)	~3.3 GPa
from Ref. 35							2.6 or 6 GPa
from Ref. 36	174	3.79	216.75	210	4.95	298.3	9.5 GPa
from Ref. 40	202(7)	2.4(6)					20–22 GPa
nc-Ga_2O_3 in glass matrix (Ref. 14)	191(5)	8.3(9)	209.5(3)				~6 GPa

In our previous pioneering work on nanocrystalline Ga_2O_3 embedded in an amorphous silica host network, we demonstrated that the β- to α-Ga_2O_3 phase transition begins at about 6 GPa in nanocrystals.[14] In that work we postulated that the host glass matrix transmits pressure to the nanocrystalline phase and that the host glass matrix is able to accommodate and relax the strains that might otherwise be found at the surface of the nanocrystals, thus increasing their stability. In this respect, the reported ~6 GPa phase transition pressure in the nanocrystalline gallium oxide lays in an intermediary range between the reported here ~3 and ~7 GPa phase transition in bulk Ga_2O_3 investigated without and with a pressure-transmitting medium, respectively.

The pressure evolution of the molar volume of the β- and the α-phase of Ga_2O_3 on compression, with and without the pressure-transmitting medium, is shown in Fig. 5. For the β-Ga_2O_3, the unit cell volume reduction was ~14% on compression from ambient pressure up to 37 GPa with nitrogen as pressure medium and ~8% for compression of the neat sample from ambient pressure up to 29 GPa. The volume reduction of the α-Ga_2O_3 was ~13% from 7.9 up to 70 GPa on compression with pressure medium and ~12% on compression of the neat sample from 3.3 up to 70 GPa.

In order to determine the bulk modulus K_0, its pressure derivative K_0' and the molar volume at ambient conditions V_0, a third-order Birch-Murnaghan[37–39] equation of state was applied:

$$P = \frac{3}{2}K_0\left[\left(\frac{V_0}{V}\right)^{7/3} - \left(\frac{V_0}{V}\right)^{5/3}\right] \times \left\{1 + \frac{3}{4}(K_0' - 4)\left[\left(\frac{V_0}{V}\right)^{2/3} - 1\right]\right\}, \qquad (1)$$

where V_0 is the volume at zero pressure, K_0 is the bulk modulus at zero pressure, and K_0' is its pressure derivative. The results of all fitting procedures are summarized in Table I. Since the K_0' values are different for the two phases, Birch Murnaghan fits with K_0' constrained to 4 were also carried out in order to give a better idea of the relative compressibility of the low- and high-pressure phases. The difference in bulk moduli of β-Ga_2O_3 and α-Ga_2O_3 obtained from compression with and without pressure-transmitting medium could be explained by an examination of the pressure evolution of the lattice parameters of both gallium oxide phases [Figs. 4(a) and 4(b)]. The lattice parameters measured in the experiment without pressure medium are, in fact, only apparent lattice parameters. Due to pseudouniaxial stress conditions experienced by the neat sample in the DAC and the directional diffraction geometry of the experiment, what is measured are the parameters normal to the DAC axis, while the lattice parameters along the compression axis behave differently. Therefore the much smaller compressibility of the parameters of the neat sample, versus the sample investigated with nitrogen, is only apparent. If the parameters were measured in all directions (e.g., in radial diffraction geometry) the real compressibility would be much higher and comparable to that of the sample studied with pressure medium.

Table I also shows a comparison of the pressure of the onset of the phase transition from our and other works as well as the results of our previous study of nanocrystalline Ga_2O_3.[14] The results reported in this work are consistent with our previous high-pressure studies of nanocomposite materials with gallium oxide nanocrystals (*nc*-Ga_2O_3) embedded in a host glass matrix, where the β-to-α phase transition was found to begin at around 6 GPa and was not completed up to 15 GPa.[14] In these studies, the estimated bulk modulus for the β-Ga_2O_3 was slightly lower than that found for bulk β-Ga_2O_3 in this work (Table I). Such difference in bulk moduli can be explained by the very different conditions of the two experiments. The *nc*-Ga_2O_3 bulk modulus was obtained for nanometer sized gallium oxide crystals embedded in an amorphous silica host network, which itself undergoes structural rearrangements resulting in significant densification on compression below 20 GPa.[16] In that work we hypothesized that the host glass matrix, which surrounds the *nc*-Ga_2O_3 is able to accommodate and relax the strains that might otherwise be found at the surface of the nanocrystals, and hence modify the actual stresses at the interface matrix-nanocrystals.

V. CONCLUSIONS

We performed *in situ* high-pressure, synchrotron x-ray diffraction studies of gallium oxide up to 70 GPa. The goal was to compare the pressure behavior of the bulk material with that of previously investigated, nanocrystalline Ga_2O_3 embedded in an amorphous silica host network, where a high-pressure phase transition was previously reported by Lipinska-Kalita *et al.*[14] Our experiment was designed to confirm the phase transition and to estimate the starting pressure of transition as well as pressure range of the expected coexistence of the two gallium oxide phases. A phase transition from a low-density monoclinic β-Ga_2O_3 into a high-density rhombohedral, corundum-type modification of α-Ga_2O_3 structure was observed. With nitrogen as a pressure medium, the transition begins at about 6.5–7 GPa and extends up to ~40 GPa. Without pressure-transmitting medium the transition begins at about 3 GPa and extends up to ~30 GPa. The comparison of the two experimental runs points to the possible role of shear stresses and deformations as the driving forces that may create defects where the transition can begin. The onset pressure of the phase transition is in agreement with recent theoretical calculations.[35,36] In both compression runs the material does not become amorphous at 70 GPa, the highest compression pressure. The diffraction patterns of the material quenched from ~70 GPa to ambient conditions indicated that the pressure-induced reconstructive modification of gallium oxide is irreversible and upon decompression only the α-Ga_2O_3 phase was present. The pressure-volume data of the two gallium oxide phases were analyzed using the Birch-Murnaghan equation of state. For the compression run with nitrogen as a pressure medium, the zero pressure bulk modulus was $K_0=199(6)$ GPa and its pressure derivative $K_0'=3.1(4)$ for the β-Ga_2O_3 and $K_0=220(9)$ GPa and its pressure derivative $K_0'=5.9(6)$ for the α-Ga_2O_3. When K_0' is constrained to 4, the bulk modulus is $K_0=184(3)$ GPa and $K_0=252(14)$ GPa for β-Ga_2O_3 and α-Ga_2O_3 respectively.

ACKNOWLEDGMENTS

We are grateful to the HPCAT staff at the APS at the Argonne National Laboratory for assistance in the measurements. This work was performed at HPCAT (Sector 16), Advanced Photon Source (APS), Argonne National Laboratory. Use of the HPCAT facility was supported by DOE-BES, DOE-NNSA (CDAC), NSF, DOD-TACOM, and the W. M. Keck Foundation. Use of the APS was supported by DOE-BES, under Contract No. DE-AC02-06CH11357.

---

*lipinska@unlv.nevada.edu

[1] H. H. Tippins, Phys. Rev. **140**, A316 (1965).

[2] M. Yamaga, E. G. Villora, K. Shimamura, N. Ichinose, and M. Honda, Phys. Rev. B **68**, 155207 (2003).

[3] N. Ueda, H. Hosono, R. Waseda, and H. Kawazoe, Appl. Phys. Lett. **70**, 3561 (1997).

[4] T. Minami, H. Yamada, Y. Kubota, and T. Miyata, Jpn. J. Appl. Phys., Part 2 **36**, L1191 (1997).

[5] L. Binet and D. Gourier, Appl. Phys. Lett. **7**, 1138 (2000).

[6] L. Binet and D. Gourier, J. Phys. Chem. Solids **59**, 1241 (1998).

[7] M. Ogita, K. Hogo, Y. Nakanishi, and Y. Hatanaka, Appl. Surf. Sci. **175-176**, 721 (2001).

[8] Z. Hajnal, J. Miro, G. Kiss, F. Reti, P. Deak, C. Herndon, and J. M. Kuperberg, J. Appl. Phys. **86**, 3792 (1999).

[9] M. Passalack, E. F. Schubet, W. S. Hobson, M. Hong, N. Moriya, S. N. G. Chu, K. Constadinidis, J. P. Mannaerts, M. L. Schnoes, and G. J. Zydzik, J. Appl. Phys. **77**, 686 (1995).

[10] E. Aubay and D. Gourier, Phys. Rev. B **47**, 15023 (1993).

[11] L. Binet and D. Gourier, J. Phys. Chem. **100**, 17630 (1996).

[12] E. A. Gonzalez, P. V. Jasen, A. Juan, S. E. Collins, M. A. Baltana, and A. L. Bonivardi, Surf. Sci. **575**, 171 (2005).

[13] R. Ceccato, R. DalMaschio, G. Mariotto, M. Montagna, F. Rossi, M. Ferrari, K. E. Lipinska-Kalita, and Y. Ohki, J. Appl. Phys. **90**, 2522 (2001).

[14] K. E. Lipinska-Kalita, B. Chen, M. B. Kruger, Y. Ohki, J. Murowchick, and E. P. Gogol, Phys. Rev. B **68**, 035209 (2003).

[15] K. E. Lipinska-Kalita, D. M. Krol, R. J. Hemley, G. Mariotto, P. E. Kalita, and Y. Ohki, J. Appl. Phys. **98**, 054302 (2005).

[16] K. E. Lipinska-Kalita, S. A. Gramsch, P. E. Kalita, and R. J. Hemley, J. Raman Spectrosc. **36**, 938 (2005).

[17] K. E. Lipinska-Kalita, G. Mariotto, P. E. Kalita, and Y. Ohki, Physica B **365**, 155 (2005).

[18] K. E. Lipinska-Kalita, O. Hemmers, P. E. Kalita, G. Mariotto, S. Gramsch, R. J. Hemley, and T. Hartmann, J. Phys. Chem. Solids (to be published).

[19] K. E. Lipinska-Kalita, P. E. Kalita, O. Hemmers, R. J. Hemley, and G. Mariotto (unpublished).

[20] P. E. Kalita, C. L. Gobin, R. J. Hemley, and K. E. Lipinska-Kalita, in Proceedings of the Stewardship Science Academic Alliance 2005 Symposium, SSAA 2005, Las Vegas, NV, http://www.orau.gov/SSAASymposium/default.htm (unpublished).

[21] K. E. Lipinska-Kalita, P. Kalita, R. J. Hemley, and C. L. Gobin, Bull. Am. Phys. Soc. **51**, R424 (2006), http://meetings.aps.org/Meeting/MAR06/Event/44114

[22] H. K. Mao, P. M. Bell, J. W. Shaner, and D. J. Steinberg, J. Appl. Phys. **49**, 3276 (1978).

[23] A. P. Hammersley, FIT 2D V10.3 Reference Manual V4.0 ESRF, Grenoble, 1998.

[24] W. Kraus and G. Nolze, POWDER CELL 2.4, FIMRT, 12489 Berlin.

[25] DIFFRACPLUS TOPAS 2.1, Bruker AXS, 2006.

[26] S. Geller, J. Chem. Phys. **33**, 676 (1966).

[27] J. Ahmen, G. Svensson, and J. Albertson, Acta Crystallogr., Sect. C: Cryst. Struct. Commun. **52**, 1336 (1996).

[28] L. Binet and D. Gourier, J. Solid State Chem. **113**, 420 (1994).

[29] M. Gauthier, High Press. Res. **22**, 779 (2002).

[30] A. Jayaraman, Rev. Mod. Phys. **55**, 65 (1983).

[31] T. S. Duffy, G. Shen, D. L. Heinz, J. Shu, Y. Ma, H. K. Mao, R. J. Hemley, and A. K. Singh, Phys. Rev. B **60**, 15063 (1999).

[32] P. Loubeyre, R. Le Toulec, D. Häusermann, M. Hanfland, R. J. Hemley, H. K. Mao, and L. W. Finger, Nature (London) **383**, 702 (1996).

[33] S. C. Schmidt, D. Schiferl, A. S. Zinn, D. D. Ragan, and D. S. Moore, J. Appl. Phys. **69**, 2793 (1991).

[34] K. E. Lipinska-Kalita, M. Pavia, and M. Nicol, J. Phys. Chem. B **109**, 19223 (2005).

[35] P. Kroll, Phys. Rev. B **72**, 144407 (2005).

[36] H. He, R. Orlando, M. A. Blanco, R. Pandey, E. Amzallag, I. Baraille, and M. Rerat, Phys. Rev. B **74**, 195123 (2006).

[37] F. D. Murnaghan, Am. J. Math. **49**, 235 (1937).

[38] F. Birch, Phys. Rev. **71**, 809 (1947).

[39] F. Birch, J. Geophys. Res. B **83**, 1257 (1978).

[40] D. Machon, P. F. McMillan, B. Xu, and J. Dong, Phys. Rev. B **73**, 094125 (2006).